

Article

On the Sintering Behavior of Nb₂O₅ and Ta₂O₅ Mixed Oxide Powders

Maureen P. Chorney¹, Kunal Mondal² , Jerome P. Downey¹ and Prabhat K. Tripathy^{3,*}

¹ Department of Materials Science and Engineering, Montana Technological University, Butte, MT 59701, USA; mchorney@mtech.edu (M.P.C.); jdowney@mtech.edu (J.P.D.)

² Materials Science and Engineering Department, Energy and Environment Science and Technology Directorate, Idaho National Laboratory, Idaho Falls, ID 83415, USA; kunal.mondal@inl.gov

³ Pyrochemistry & Molten Salt Systems Department, Fuel Cycle Science and Technology Division, Nuclear Science and Technology Directorate, Idaho National Laboratory, Idaho Falls, ID 83415, USA

* Correspondence: prabhat.tripathy@inl.gov; Tel.: +1-208-533-7193

Abstract: A mixed oxide system consisting of Nb₂O₅ and Ta₂O₅, was subjected to annealing in air/hydrogen up to 950 °C for 1–4 h to study its sintering behavior. The thermogravimetric–differential scanning calorimetry (TGA–DSC) thermograms indicated the formation of multiple endothermic peaks at temperatures higher than 925 °C. Subsequently, a 30% Ta₂O₅ and 70% Nb₂O₅ (mol%) pellet resulted in good sintering behavior at both 900 and 950 °C. The scanning electron microscope (SEM) images corroborated these observations with necking and particle coarsening. The sintered pellets contained a 20.4 and 20.8% mixed oxide (Nb₄Ta₂O₁₅) phase, along with Ta₂O₅ and Nb₂O₅, at both 900 and 950 °C, indicating the possibility of the formation of a solid solution phase. In situ high-temperature X-ray diffraction (XRD) scans also confirmed the formation of the ternary oxide phase at 6 and 19.8% at 890 and 950 °C, respectively. The Hume–Rothery rules could explain the good sintering behavior of the Ta₂O₅ and Nb₂O₅ mixed oxides. An oxide composition of 30% Ta₂O₅ and 70% Nb₂O₅ (mol%) and a sintering temperature of 950 °C appeared adequate for fabricating well-sintered oxide precursors for subsequent electrochemical polarization studies in fused salts.

Keywords: tantalum pentoxide; niobium pentoxide; energy materials; oxide precursor; sintering; green manufacturing



Citation: Chorney, M.P.; Mondal, K.; Downey, J.P.; Tripathy, P.K. On the Sintering Behavior of Nb₂O₅ and Ta₂O₅ Mixed Oxide Powders. *Materials* **2022**, *15*, 5036. <https://doi.org/10.3390/ma15145036>

Academic Editors: Dina Dudina and Arina V. Ukhina

Received: 17 May 2022

Accepted: 14 July 2022

Published: 20 July 2022

Publisher's Note: MDPI stays neutral with regard to jurisdictional claims in published maps and institutional affiliations.



Copyright: © 2022 by the authors. Licensee MDPI, Basel, Switzerland. This article is an open access article distributed under the terms and conditions of the Creative Commons Attribution (CC BY) license (<https://creativecommons.org/licenses/by/4.0/>).

1. Introduction

Transition metals and their alloys, compounds, and large complexes containing transition metals are widely used for a variety of purposes ranging from specialized high-temperature applications to more common uses, such as in catalysis, materials synthesis, photochemistry, biological systems, environment cleaning, and electronics. The fabrication of transition-metal-based functional oxides and hydroxides from aqueous metal-oxo cluster precursors and electrochemical routes has opened up numerous opportunities for the development of sustainable green chemistry. These suitable chemistries have led to the development of new materials for energy generation and storage, data storage, and many other potential applications. Although metal-oxo cluster chemistries, pertaining to group V and VI elements, have been widely reported, some of the issues pertaining to ligand dynamics, post-synthesis ligand exchange, and cluster stability have largely remained unresolved [1]. While the controlled electrochemical synthesis approach has limited benefits, researchers have been unable to resolve some of the difficulties related to synthesis because of the prevalence of incomplete solid-state diffusion kinetics [2]. Like the transition metal-oxo clusters, researchers have also developed rare-earth metal hexacyanoferrates for electrocatalysis and adsorbents for heavy ion removal applications [2–7]. In addition to the transition and rare-earth metal complexes, hexacyanoferrate simple oxides are also widely used in many technologies.

Many sectors use two of the group V oxides, Ta₂O₅ and Nb₂O₅. Because of its excellent dielectric properties, Ta₂O₅ is used in dynamic random access memory chips, field effect transistors, thin-film electroluminescence devices, biological and chemical sensors, antireflection coatings for silicon solar cells, charge-coupled devices, corrosion-resistant materials, optical wave guides, and thin-film resistors [8]. Nb₂O₅, on the other hand, exhibits strong redox abilities and unique Lewis and Brønsted acid sites, and as a result has been used for photocatalytic activities [9]. Another application of Nb₂O₅ has been in the fabrication of resistive random memory access devices because of the dependence of its dual electrical response of memory and threshold switching behaviors on oxygen contents resistive to random memory access devices [10]. Nb₂O₅ is routinely used in gas sensors, catalysis, optical and electrochromic devices, solid-state electrochemical devices, and biocompatible prostheses [11]. Because of the similarity in their chemical and structural properties, Ta₂O₅ and Nb₂O₅ mixed oxides have been used as coatings and thin films to either enhance the dielectric permittivity of Ta₂O₅ or the band gap of Nb₂O₅ [12]. Forming a mixed oxide phase, a solid solution of Nb₂O₅ and Ta₂O₅ (NbTaO₅, (Ta_{1-x}Nb_x)₂O₅(Ta_{1-x}Nb_x)₂O₅, x = 0.02–0.07) is advantageous in terms of having a lower leakage current and enhanced dielectric permittivity in the device [12,13]. Fine (micron-sized) Nb₂O₅ and Ta₂O₅ powders formed reactive thermites and composites with nanosized aluminum, where the oxide mixture acted as the gasless oxidizer and the metal (aluminum) was a fuel [14].

Binary alloys of niobium and tantalum can serve as anticorrosion coatings (for CoCr alloys in the biomedical industry) [15] in the fabrication of high-entropy shape memory and superconducting alloys [16–18]. These applications employ a melting-cum-remelting process to make a homogeneous alloy from which the components are fabricated. In recent years, researchers have developed a novel electrochemical process to fabricate many metallic materials, both metals and alloys, from their oxide and mixed oxide intermediates. Although both Ta₂O₅ and Nb₂O₅, individually, have been successfully converted to tantalum and niobium, respectively, in molten salts [19–21], studies on the co-reduction of the mixed oxides in molten salts to form the binary (NbTa) alloy are absent in the literature. Both Nb₂O₅ and Ta₂O₅ were mixed with other oxides (TiO₂, ZrO₂, and HfO₂) to form high-entropy alloys, consisting of titanium–niobium–tantalum–zirconium and titanium–niobium–tantalum–zirconium–hafnium, in a calcium chloride melt [22]. However, no studies appear to have reported on the formation of the binary alloys from their mixed oxide precursors. Three types of salts (LiCl–Li₂O, CaCl₂–CaO, and eutectic CaCl₂–NaCl) have been used to electrochemically reduce metal oxides to their metallic constituent. Each electrolyte system offers a set of advantages and disadvantages. CaCl₂ provides two distinct advantages: the relatively higher solubility of the oxide ions in calcium chloride and enhanced reduction kinetics, thereby decreasing the overall reduction time. The objective of the present study was to examine the co-reduction behavior of the mixed oxides in a calcium chloride melt. The experimental research was divided into two parts: (1) the preparation, evaluation, and characterization of mixed oxide precursor; (2) the electrochemical reduction of precursor materials prepared under a set of optimum conditions. The present manuscript describes the experimental results pertaining to the preparation and characterization of mixed oxide precursors. The experimental work consisted of the mixing and homogenization of Ta₂O₅ and Nb₂O₅, thermal analyses of the powder, the pelletization of the homogenized powder, the sintering of the mixed powder, a study of the powder's morphology using a scanning electron microscope, and phase analyses of the heat-treated powders via room- and high-temperature X-ray diffraction.

2. Materials and Methods

2.1. Materials

High-purity and finely powdered tantalum pentoxide (Ta₂O₅, Sigma-Aldrich (St. Louis, MO, USA) 99.99% trace metals basis, <20 μm) and niobium pentoxide (Nb₂O₅, Sigma-Aldrich, 99.9% trace metals basis, –325 mesh) were used as the starting materials. Polyvinyl

alcohol/[poly (vinyl butyral-co-vinyl alcohol-co-vinyl acetate)] (PVB/PVA), Sigma-Aldrich, average MW = 50,000–80,000 by gel permeation chromatography (GPC) and poly (ethylene glycol, PEG, Sigma-Aldrich, average MW = 200) were used as the binder to prepare the powder mixture. Finally, the powder mixture was homogenized in a ball miller for 4 h and the slurry was dried (under a heat lamp) over a period of ~36 h.

2.2. Equipment

A thermogravimetric analyzer (simultaneous TGA–DSC, SDT Q600, TA instruments, New Castle, DE, USA) performed the initial heat treatment of the milled (mixed) oxide powder. An MTI 1100X Series tube furnace (MTI corporation, Richmond, CA, USA) sintered the pelletized powder mixture. An X-ray diffraction unit with PDXL (Rigaku, Japan) and JADE software (MDI, Hibbing, MN, USA) programs analyzed the diffraction patterns. A small furnace containing a platinum tray and a scintillation detector was used to collect X-ray diffraction (XRD, Rigaku Ultima IV diffractometer) data. A D/teX Ultra detector (Rigaku, Tokyo, Japan) recorded the room-temperature XRD patterns of the sintered pellets. A scanning electron microscope (MIRA3 TESCAN SEM, TESCAN USA, Inc., Warrendale, PA, USA) with an energy-dispersive X-ray (EDS) analysis attachment was used to examine the sintered pellet morphologies.

2.3. Procedure

Calculated quantities of Ta₂O₅ and Nb₂O₅ powders were mixed and homogenized in an agate mortar and pestle. About 8–15 mg powders were placed in an alumina crucible, which in turn was loaded into the simultaneous TGA–DSC unit. The mixed powder was heated at 5 °C/min to a maximum temperature of 1150 °C to record the endo- and exothermic peaks. This heating was performed under a continuous argon flow. Depending on the thermogram results, a few powder compositions were formulated to record the exothermic and endothermic peaks and percentage mass loss. A laboratory hydraulic pressing unit was used to pelletize the milled powder. The powder was compacted into 13 mm dia. pellets in a steel die by applying around 29–29.6 MPa of pressure. The green pellets were subsequently loaded into an alumina boat and heated in air/hydrogen up to the desired temperatures (up to 950 °C) for fixed durations (1–4 h). The sintered pellets were subsequently evaluated with respect to their phase compositions and morphological features with a 10 °C/min heating rate to record the in situ high-temperature XRD data. The temperature controller was set up to hold at the set temperature for 5 min in order to have a sample with a uniform temperature across its surface. The detailed information pertaining to the preparation of samples and experimental procedure is described elsewhere [23].

3. Results and Discussion

3.1. TGA–DSC Studies

A 50:50 (mass%) composition of the mixed powder showed three endothermic peaks, at 925.62 °C, 1006.1 °C, and 1036.66 °C, respectively. The Ta₂O₅-Nb₂O₅ binary phase diagram indicates the formation of a solid solution in a composition with about 26 mol% Ta₂O₅ [24]. This is why it was decided to investigate a few compositions around 26 mol% to observe the formation of any solid solution and the ternary oxide composition that might influence the subsequent electrochemical reduction step. A composition of 26 to 74 mol% Ta₂O₅ and Nb₂O₅, respectively, showed a single endothermic peak at 923.75 °C. Similarly, two more compositions of 21 to 79 mol% and 31 to 69 mol% Ta₂O₅-Nb₂O₅ showed endothermic peaks at just one temperature (924.54 °C) (Figure 1). The TGA indicated insignificant weight loss values (1.48–2.04%) (Figure 2). These studies indicated that perhaps a temperature of around or higher than 925 °C is needed to obtain an adequately sintered pellet.

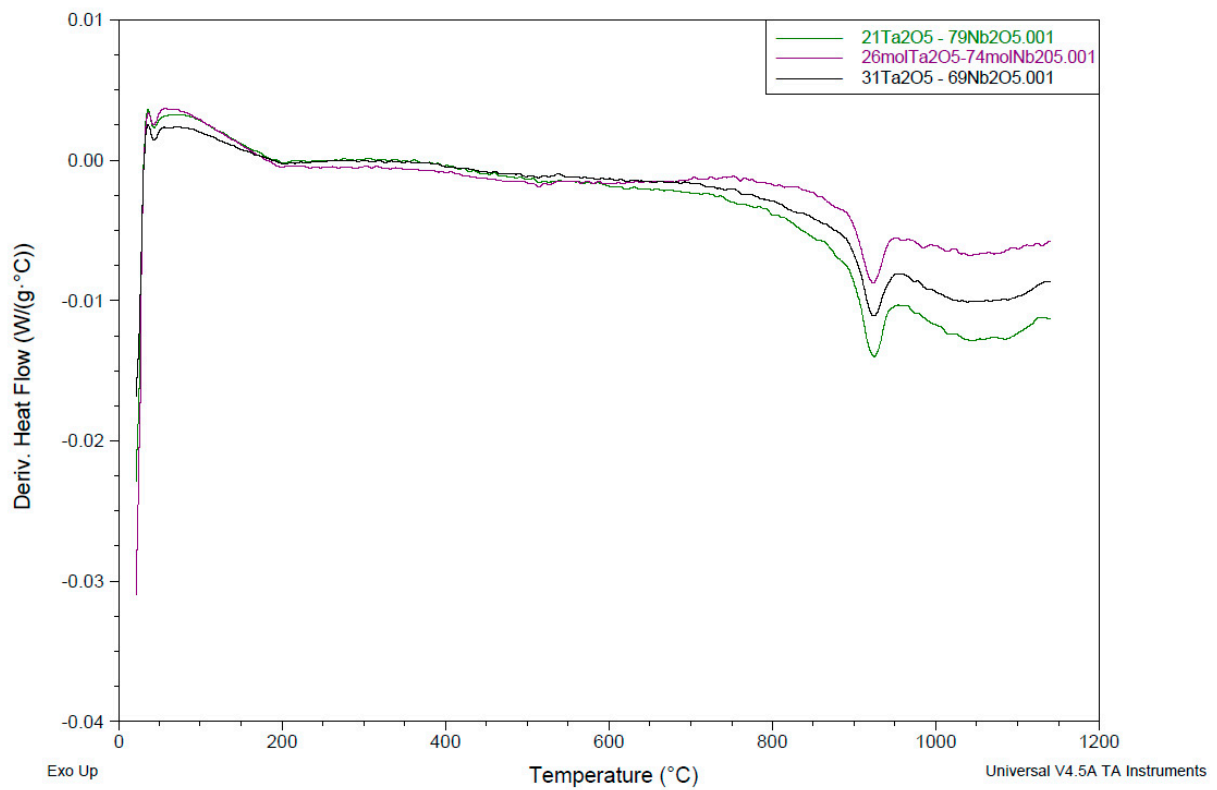


Figure 1. DSC scans of three Ta₂O₅-Nb₂O₅ compositions (green: 21 Ta₂O₅ to 79 Nb₂O₅; violet: 31 Ta₂O₅ to 69 Nb₂O₅; grey: 26 Ta₂O₅ to 74 Nb₂O₅; all concentrations are in mol%).

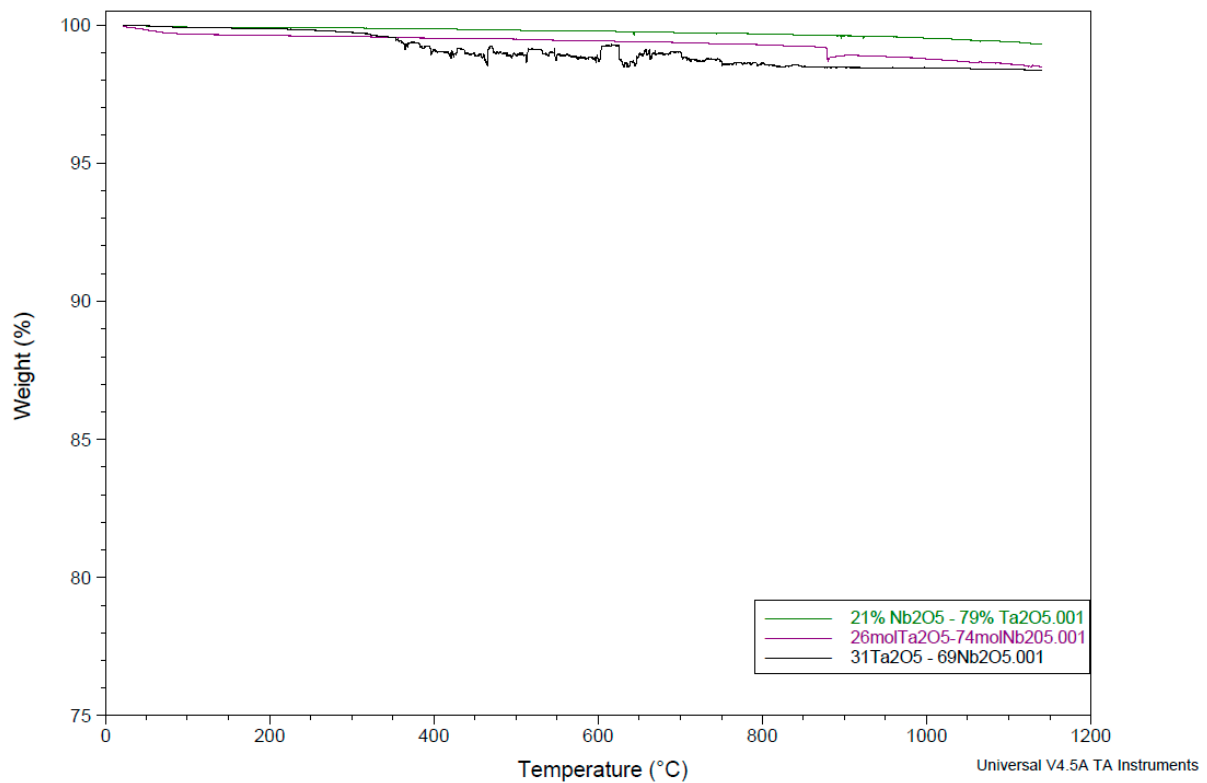


Figure 2. TGA scans of three Ta₂O₅-Nb₂O₅ compositions (green: 21 Ta₂O₅ to 79 Nb₂O₅; violet: 31 Ta₂O₅ to 69 Nb₂O₅; grey: 26 Ta₂O₅ to 74 Nb₂O₅; all concentrations are in mol%) showing weight loss (%).

3.2. Morphology of the Sintered Pellets

Based on the TGA–DSC studies, a 30 mol% Ta₂O₅ to 70 mol% Nb₂O₅ composition was used to prepare the mixed oxide pellets from the homogenized powder. The green pellets were subsequently heated at two different temperatures (900 and 950 °C, respectively) to observe the overall sintering behavior of the mixed powders. Figure 3 shows scanning electron microscope images of the pellets sintered at 900 and 950 °C. Both pellets showed very good sintering behavior consisting of necking (initial sintering stage) and reductions in porosity and particle size coarsening. As expected, the heat-treated pellet at 950 °C showed a better degree of sintering as compared to the pellet, which was sintered at 900 °C. Some of the scattered darker pieces were alumina, which may have come from the grinding media. The EDS analysis, as expected, showed tantalum, niobium, and oxygen as major peaks along with traces of aluminum and carbon due to the contamination and use of a carbon tape. Based on the morphological features, precursor materials were prepared at 950 °C for their subsequent conversion to the binary (metallic) alloy.

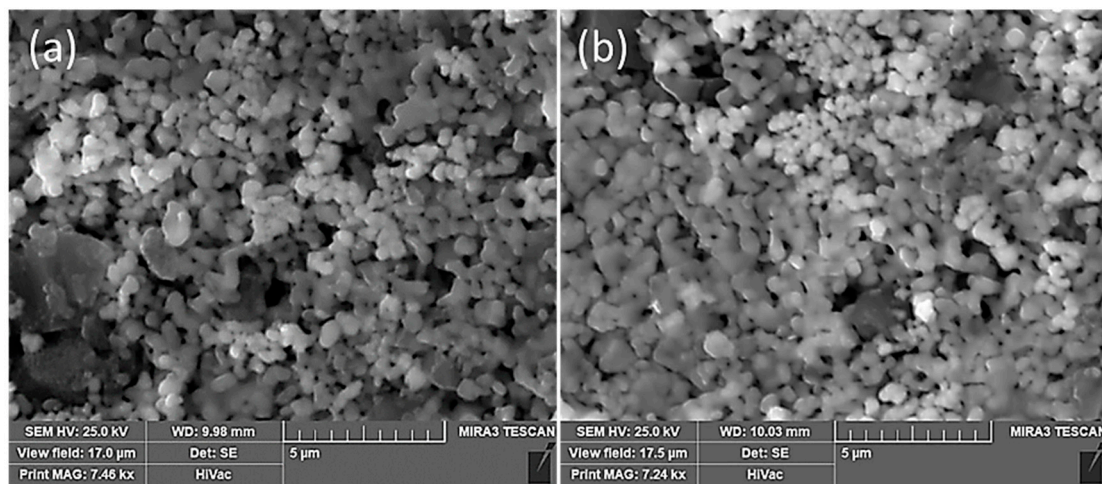
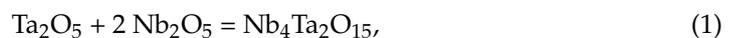


Figure 3. Scanning electron microscope images of sintered pellets: (a) 900 °C; (b) 950 °C.

3.3. Phase Identification: Room-Temperature X-ray Diffraction Patterns

The XRD data indicated that both oxide phases (Ta₂O₅ and Nb₂O₅) were present. In addition to the two binary phases, the formation of a mixed oxide phase (Nb₄Ta₂O₁₅) could also be identified (Equation (1)):



Contrary to these findings, Fazio et al. [25] could not detect any ternary oxide when they doped amorphous Ta₂O₅ thin films with Nb₂O₅ and sintered the resultant product in air up to 900 °C for 10 h. According to these authors, both Ta₂O₅ and Nb₂O₅ are quite stable when forming any ternary oxides. They concluded that in the absence of any ternary oxide phase, the dopant (Nb₂O₅) acted as an amorphizing agent that increased the thermal stability of the Ta₂O₅ thin films [25]. The new phase (Nb₄Ta₂O₁₅) did not have any reported reference intensity ratio (RIR) values. This was why the diffraction patterns were analyzed with the JADE software to estimate the RIR values. In order to obtain the relative weight percentages of the compounds within the sample, it is necessary to assign a RIR value to derive the quantitative information. Three RIR values, 2.8 (Nb₂O₅), 8.2 (Ta₂O₅), and their mean (5.5), were selected. Tables 1–6 list the quantitative phase analyses of the pellets sintered at 900 and 950 °C with three sets of RIR values in each case.

With a lower RIR value, the quantity of niobium tantalum oxide was as high as 56.1% of the total phase composition. A relatively larger peak with a small RIR value indicates a larger quantity of that particular phase. In comparison, a relatively larger peak with a larger RIR value will result in a smaller quantity of the phase of interest as the larger

RIR value indicates that the peak of the particular phase is naturally higher than that of the reference standard (corundum). The largest RIR indicated that 20.4% of the sample consisted of the ternary oxide phase.

Table 1. Quantitative XRD (phase) analysis results (whole pattern fitting (WPF) combined with RIR) of a 70 mol% Nb₂O₅ to 30 mol% Ta₂O₅ pellet at 900 °C (Nb₄Ta₂O₁₅, RIR = 2.8).

Phase Name	Formula	RIR	DB Card No.	Content	Total Ta _x Nb _y O _z
Tantalum Oxide	Ta ₂ O ₅	8.20	01-025-0922	13.6	
Niobium Oxide	Nb ₂ O ₅	2.79	01-071-1169	30.3	
Niobium Tantalum Oxide	Nb ₄ Ta ₂ O ₁₅	2.80	01-071-4513	56.1	
				100.0	56.1

Table 2. Quantitative XRD (phase) analysis results (WPF, combined with RIR) of a 70 mol% Nb₂O₅ to 30 mol% Ta₂O₅ pellet at 900 °C (Nb₄Ta₂O₁₅, RIR = 5.5).

Phase Name	Formula	RIR	DB Card No.	Content	Total Ta _x Nb _y O _z
Tantalum Oxide	Ta ₂ O ₅	8.20	01-025-0922	25.2	
Niobium Oxide	Nb ₂ O ₅	2.79	01-071-1169	46.8	
Niobium Tantalum Oxide	Nb ₄ Ta ₂ O ₁₅	5.50	01-071-4513	28.0	
				100.0	28.0

Table 3. Quantitative XRD (phase) analysis results (WPF, combined with RIR) of a 70 mol% Nb₂O₅ to 30 mol% Ta₂O₅ pellet at 900 °C (Nb₄Ta₂O₁₅, RIR = 8.2).

Phase Name	Formula	RIR	DB Card No.	Content	Total Ta _x Nb _y O _z
Tantalum Oxide	Ta ₂ O ₅	8.20	01-025-0922	27.7	
Niobium Oxide	Nb ₂ O ₅	2.79	01-071-1169	51.9	
Niobium Tantalum Oxide	Nb ₄ Ta ₂ O ₁₅	8.20	01-071-4513	20.4	
				100.0	20.4

Table 4. Quantitative XRD (phase) analysis results (WPF, combined with RIR) of a 70 mol% Nb₂O₅ to 30 mol% Ta₂O₅ pellet at 950 °C (Nb₄Ta₂O₁₅, RIR = 2.8).

Phase Name	Formula	RIR	DB Card No.	Content	Total Ta _x Nb _y O _z
Tantalum Oxide	Ta ₂ O ₅	8.20	01-025-0922	21.9	
Niobium Oxide	Nb ₂ O ₅	2.79	01-071-1169	35.8	
Niobium Tantalum Oxide	Nb ₄ Ta ₂ O ₁₅	2.80	01-071-4513	42.2	
				99.9	42.2

Table 5. Quantitative XRD (phase) analysis results (WPF, combined with RIR) of a 70 mol% Nb₂O₅ to 30 mol% Ta₂O₅ pellet at 950 °C (Nb₄Ta₂O₁₅, RIR = 5.5).

Phase Name	Formula	RIR	DB Card No.	Content	Total Ta _x Nb _y O _z
Tantalum Oxide	Ta ₂ O ₅	8.20	01-025-0922	29.6	
Niobium Oxide	Nb ₂ O ₅	2.79	01-071-1169	44.0	
Niobium Tantalum Oxide	Nb ₄ Ta ₂ O ₁₅	5.50	01-071-4513	26.3	
				99.9	26.3

Table 6. Quantitative XRD (phase) analysis results (WPF, combined with RIR) of a 70 mol% Nb₂O₅ to 30 mol% Ta₂O₅ pellet at 950 °C (Nb₄Ta₂O₁₅, RIR = 8.2).

Phase Name	Formula	RIR	DB Card No.	Content	Total Ta _x Nb _y O _z
Tantalum Oxide	Ta ₂ O ₅	8.20	01-025-0922	24.9	
Niobium Oxide	Nb ₂ O ₅	2.79	01-071-1169	54.3	
Niobium Tantalum Oxide	Nb ₄ Ta ₂ O ₁₅	8.20	01-071-4513	20.8	
				100.0	20.8

A similar phase distribution was observed while analyzing a pellet sintered at 950 °C. Although the overall quantity of niobium tantalum oxide (RIR = 2.8) was slightly lower than the value at 900 °C, at 42.2% compared to 56.1%, the 5.5 and 8.2 RIR values produced similar results at both sintering temperatures. The amounts of mixed oxide phases at 900 and 950 °C for an RIR value of 5.5 were 28 and 26.2%, respectively. Similarly, for an RIR value of 8.2, the mixed oxide phases were 20.4 and 20.8% at 900 and 950 °C, respectively.

The quantitative phase analysis data from the room-temperature XRD scans indicated mixed oxide compositions of 20.4 and 20.8% at 900 and 950 °C, respectively. The binary phase diagram indicated the possibility of the formation of a solid solution in these compositions.

3.4. Phase Identification: High-Temperature X-ray Diffraction

In situ XRD patterns were recorded at four different temperatures (25, 890, 925, and 950 °C, respectively). The quantitative data for different RIR values are presented in Tables 7–9. As expected, the fraction of the mixed oxide phase was higher at 950 °C (19.8–34.4%) than at 890 °C (6.0–13.2%). A comparison between the room- and high-temperature XRD data for the mixed oxide phase indicated an interesting pattern. While there was no change between the values obtained at 900 and 950 °C (at room temperature), the fraction registered a somewhat lower value at 950 °C (42.2%) than at 900 °C (56.1%). Figure 4 shows an overlay of the diffraction patterns recorded at 890 °C and 925 °C, respectively. These results indicated a definitive trend in the mixed oxide content, with an increase in temperature from 890 to 925 °C. Although the initial percentages of tantalum pentoxide and niobium pentoxide appeared to be skewed at 25 °C (Tables 7–9), the subsequent values showed consistencies at other temperatures, with the values decreasing as the formation of the Nb₄Ta₂O₁₅ phase increased. A minimal amount of mixed oxide was detected at 890 °C, but the composition changed dramatically when the temperature was increased by 35 °C. The amount of Nb₄Ta₂O₁₅ decreased as the temperature was increased to 950 °C, which could have resulted because of the presence of metastable phases at 925 °C, which became unstable at higher temperatures. Alternatively, the decrease might have happened as the result of an error in the RIR value.

Mohanty et al. [24] investigated the phase equilibria in the mixed oxide system in a bid to determine the discrepancies reported in the literature. They prepared the mixed oxide systems by heating the mixtures of Ta₂O₅ and Nb₂O₅ in oxygen, argon, and an argon–air mixture (80% Ar–20% oxygen) to determine the effects of such treatments on the stoichiometry and structure of the base materials. They did observe the formation of α-Ta₂O₅ phase and 2Nb₂O₅·Ta₂O₅ compound at 1435 °C when the Ta₂O₅ content was higher than 36% [26]. They also reported the formation of α-Nb₂O₅ and β-Ta₂O₅ at a slightly lower temperature range (1200–1300 °C) [24]. Some other authors have also reported similar studies [27]. Mohanty et al. also reported high-temperature XRD measurements. Their studies indicated the formation of a two-phase region (α-Ta₂O₅ + β-Ta₂O₅) in the composition range of 50–100% Ta₂O₅ [24].

As stated earlier, the focus in the present investigation was to prepare a stable mixed oxide precursor (which should not undergo disintegration during the subsequent electrochemical polarization in calcium chloride melt at ~800 °C) and not the detailed phase

analysis. Unlike in other (reported) studies, where the mixed oxide compositions were kept at 1000 °C for a duration of 24 h [24], in the present studies the temperature and duration were <1000 °C and up to 4 h, respectively. Like other studies, the present study also confirmed the presence of the ternary oxide ($\text{Nb}_4\text{Ta}_2\text{O}_{15}$) along with the other two oxides (Ta_2O_5 and Nb_2O_5) at all temperatures, albeit after heating for a relatively fewer number of hours.

Table 7. Quantitative phase analysis results (WPF) from the high-temperature XRD scans of a 30 mol% Ta_2O_5 to 70 mol% Nb_2O_5 pellet ($\text{Nb}_4\text{Ta}_2\text{O}_{15}$ RIR = 2.8).

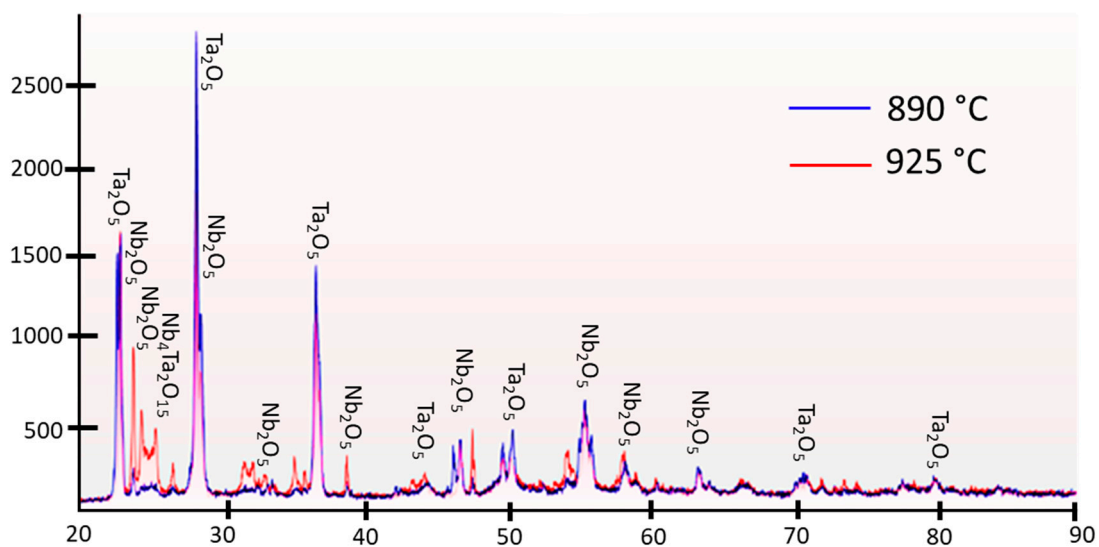
°C	Phase Name	Formula	RIR	PDF No	Content	Total $\text{Ta}_x\text{Nb}_y\text{O}_z$
25	Tantalum Oxide	Ta_2O_5	8.20	00-025-0922	60.3	—
	Niobium Oxide	Nb_2O_5	2.79	00-030-0873	39.7	
					100.0	
890	Tantalum Oxide	Ta_2O_5	8.20	00-025-0922	25.4	13.2
	Niobium Oxide	Nb_2O_5	2.79	00-030-0873	61.4	
	Niobium Tantalum Oxide	$\text{Nb}_4\text{Ta}_2\text{O}_{15}$	2.80	00-015-0114	13.2	
					100.0	
925	Tantalum Oxide	Ta_2O_5	8.20	00-025-0922	31.0	18.3
	Niobium Oxide	Nb_2O_5	2.79	00-030-0873	50.7	
	Niobium Tantalum Oxide	$\text{Nb}_4\text{Ta}_2\text{O}_{15}$	2.80	00-015-0114	18.3	
					100.0	
950	Tantalum Oxide	Ta_2O_5	8.20	00-025-0922	34.7	19.8
	Niobium Oxide	Nb_2O_5	2.79	00-030-0873	45.5	
	Niobium Tantalum Oxide	$\text{Nb}_4\text{Ta}_2\text{O}_{15}$	2.80	00-015-0114	19.8	
					100.0	

Table 8. Quantitative phase analysis results (WPF) from the high-temperature XRD scans of a 30 mol% Ta_2O_5 to 70 mol% Nb_2O_5 pellet ($\text{Nb}_4\text{Ta}_2\text{O}_{15}$ RIR = 5.5).

°C	Phase Name	Formula	RIR	PDF No	Content	Total $\text{Ta}_x\text{Nb}_y\text{O}_z$
25	Tantalum Oxide	Ta_2O_5	8.20	00-025-0922	60.3	—
	Niobium Oxide	Nb_2O_5	2.79	00-030-0873	39.7	
					100.0	
890	Tantalum Oxide	Ta_2O_5	8.20	00-025-0922	36.2	8.0
	Niobium Oxide	Nb_2O_5	2.79	00-030-0873	55.8	
	Niobium Tantalum Oxide	$\text{Nb}_4\text{Ta}_2\text{O}_{15}$	5.50	00-015-0114	8.0	
					100.0	
925	Tantalum Oxide	Ta_2O_5	8.20	00-025-0922	42.3	39.7
	Niobium Oxide	Nb_2O_5	2.79	00-030-0873	18.0	
	Niobium Tantalum Oxide	$\text{Nb}_4\text{Ta}_2\text{O}_{15}$	5.50	00-015-0114	39.7	
					100.0	
950	Tantalum Oxide	Ta_2O_5	8.20	00-025-0922	41.2	34.4
	Niobium Oxide	Nb_2O_5	2.79	00-030-0873	24.3	
	Niobium Tantalum Oxide	$\text{Nb}_4\text{Ta}_2\text{O}_{15}$	5.50	00-015-0114	34.4	
					99.9	

Table 9. Quantitative phase analysis results (WPF) from the high-temperature XRD scans of a 30 mol% Ta₂O₅ to 70 mol% Nb₂O₅ pellet (Nb₄Ta₂O₁₅ RIR = 8.2).

°C	Phase Name	Formula	RIR	PDF No	Content	Total Ta _x Nb _y O _z
25	Tantalum Oxide	Ta ₂ O ₅	8.20	00-025-0922	60.3	—
	Niobium Oxide	Nb ₂ O ₅	2.79	00-030-0873	39.7	
					100.0	
890	Tantalum Oxide	Ta ₂ O ₅	8.20	00-025-0922	36.2	6.0
	Niobium Oxide	Nb ₂ O ₅	2.79	00-030-0873	55.8	
	Niobium Tantalum Oxide	Nb ₄ Ta ₂ O ₁₅	8.20	00-015-0114	8.0	
					100.0	
925	Tantalum Oxide	Ta ₂ O ₅	8.20	00-025-0922	42.3	26.5
	Niobium Oxide	Nb ₂ O ₅	2.79	00-030-0873	18.0	
	Niobium Tantalum Oxide	Nb ₄ Ta ₂ O ₁₅	8.20	00-015-0114	39.7	
					100.0	
950	Tantalum Oxide	Ta ₂ O ₅	8.20	00-025-0922	41.2	21.1
	Niobium Oxide	Nb ₂ O ₅	2.79	00-030-0873	24.3	
	Niobium Tantalum Oxide	Nb ₄ Ta ₂ O ₁₅	8.20	00-015-0114	34.4	
					100.0	

**Figure 4.** Overlay of the diffraction patterns recorded at two different temperatures (890 and 925 °C, respectively) for a 70 mol% Ta₂O₅ and 30 mol% Nb₂O₅ pellet, respectively.

4. Conclusions

Mixed oxides, containing Ta₂O₅ and Nb₂O₅ in different molar ratios, were subjected to thermal treatment in a TGA–DSC setup up to a maximum of 1150 °C. The recorded thermograms indicated sintering behavior at temperatures over 850 °C. The morphology of the sintered powders indicated good sintering behavior at or above 900 °C for a 30 mol% Ta₂O₅ to 70 mol% Nb₂O₅ composition. The Hume–Rothery rules (identical ionic radii, valence states, electronegativity, and crystal structure) could explain the good sintering behavior of the Ta₂O₅ and Nb₂O₅ mixed oxides. Furthermore, 950 °C is adequate to prepare the mixed oxide precursors (30 mol% Ta₂O₅ to 70 mol% Nb₂O₅) with good mechanical integrity. Both the room- and high-temperature XRD studies indicated the formation of a ternary oxide phase. The quantitative determination of the mixed oxide phase is dependent on the relative intensity response (RIR) value. The sintered pellets, upon immersion into a pool of molten calcium chloride at 850 °C, did not form any surface. Two specific

characteristics (percentage open porosity and good mechanical strength) were observed to be the critical parameters for the preparation of the mixed oxide precursors for their subsequent conversion to the binary metallic alloys.

Author Contributions: Experimentation, M.P.C.; conceptualization and design of experiments, P.K.T.; data interpretation, K.M.; interpretation of XRD results, J.P.D. All authors have read and agreed to the published version of the manuscript.

Funding: Laboratory Directed Research and Development Project (Project Id.: 16-003), Idaho National Laboratory, U.S. Department of Energy.

Institutional Review Board Statement: The institutional approval number is: INL/JOU-22-66994.

Informed Consent Statement: Not applicable.

Data Availability Statement: Not applicable.

Acknowledgments: The authors express their sincere thanks to the Idaho National Laboratory Directed Research and Development Program under Department of Energy Idaho Operation Office for supporting the research work. The manuscript was authorized by Battelle Energy Alliance LLC under the contract no. DE-AC07-051D14517 with the U.S. Department of Energy for publication. The publisher, by accepting the manuscript for publication, acknowledges that the U.S. government retains a non-exclusive, paid-up, irrevocable, worldwide license to publish or reproduce the published form of this manuscript or allow others to do so for U.S. government purposes.

Conflicts of Interest: The authors declare that they have no known competing financial interests or personal relationships that could have appeared to influence the work reported in the present manuscript.

Disclaimer: The information was prepared as an account of the work sponsored by an agency of the U.S. government. Neither the U.S. government nor any agency thereof, nor any of their employees, makes any warranty, expressed or implied, or assumes any legal liability or responsibility for the accuracy, completeness, or usefulness of any information, apparatus, product, or process disclosed, or represents that its use would not infringe on privately owned rights. References herein to any specific commercial product, process, or service by trade name, trademark, manufacturer, or otherwise does not necessarily constitute or imply its endorsement, recommendation, or favoring by the U.S. government or any agency thereof. The views and opinions of the authors expressed herein do not necessarily state or reflect those of the U.S. government or any agency thereof.

References

1. Gunay, A.; Theopold, K.H. C–H bond activations by metal oxo compounds. *Chem. Rev.* **2010**, *110*, 1060–1081. [[CrossRef](#)] [[PubMed](#)]
2. Devadas, B.; Madhu, R.; Chen, S.-M.; Yeh, H.-T. Controlled electrochemical synthesis of new rare earth metal lutetium hexacyanoferrate on reduced graphene oxide and its application as a salicylic acid sensor. *J. Mater. Chem. B* **2014**, *2*, 7515–7523. [[CrossRef](#)] [[PubMed](#)]
3. Sitnikova, N.A.; Komkova, M.A.; Khomyakova, I.V.; Karyakina, E.E.; Karyakin, A.A. Transition metal hexacyanoferrates in electrocatalysis of H₂O₂ reduction: An exclusive property of Prussian blue. *Anal. Chem.* **2014**, *86*, 4131–4134. [[CrossRef](#)] [[PubMed](#)]
4. Wang, J.; Zhuang, S.; Liu, Y. Metal hexacyanoferrates-based adsorbents for cesium removal. *Coord. Chem. Rev.* **2018**, *374*, 430–438. [[CrossRef](#)]
5. Bohara, B.B.; Batra, A.K.; Arun, K.J.; Aggarwal, M.D.; Farley, C. Fabrication and characterization of polyvinylidene fluoride trifluoroethylene/samarium oxide (Sm₂O₃) nanocomposite films. *Adv. Sci. Eng. Med.* **2017**, *9*, 1–6. [[CrossRef](#)]
6. Wooles, A.J.; Cooper, O.J.; McMaster, J.; Lewis, W.; Blake, A.J.; Liddle, S.T. Synthesis and characterization of dysprosium and lanthanum bis(iminophosphorano)methanide and -methanediide complexes. *Organometallics* **2010**, *29*, 2315–2321. [[CrossRef](#)]
7. Mautner, F.A.; Bierbaumer, F.; Gyurkac, M.; Fischer, R.C.; Torvisco, A.; Massoud, S.S.; Vicente, R. Synthesis and characterization of lanthanum(III) complexes containing 4,4,4-trifluoro-1-(naphthalen-2yl)butane-1,3-dionate. *Polyhedron* **2020**, *179*, 114384. [[CrossRef](#)]
8. Chaneliere, C.; Autran, J.L.; Devine, R.A.B.; Balland, B. Tantalum pentoxide (Ta₂O₅) thin films for advanced dielectric applications. *Mater. Sci. Eng. R. Rep.* **1998**, *22*, 269–322. [[CrossRef](#)]
9. Su, K.; Liu, H.; Fornasiero, P.; Wang, F. Nb₂O₅-based photocatalysts. *Adv. Sci.* **2021**, *8*, 2003156. [[CrossRef](#)]
10. Aziz, J.; Kim, H.; Rehman, S.; Kadam, K.D.; Patil, H.; Aftab, S.; Khan, M.F.; Kim, D.-K. Discrete memristive levels and logic gate applications of Nb₂O₅ devices. *J. Alloys Compd.* **2021**, *879*, 1603885. [[CrossRef](#)]

11. Minagar, S.; Berndt, C.C.; Wen, C. Fabrication and characterization of nanoporous niobia, and nanotubular tantalum, titania and zirconia via anodization. *J. Funct. Biomater.* **2015**, *6*, 153–170. [[CrossRef](#)]
12. Kukli, K.; Ritala, M.; Leskela, M. Properties of atomic layer deposited $(\text{Ta}_{1-x}\text{Nb}_x)_2\text{O}_5$ solid solution films and Ta_2O_5 - Nb_2O_5 nanolaminates. *J. Appl. Phys.* **1999**, *86*, 5656. [[CrossRef](#)]
13. Clima, S.; Pourtois, G.; Van Elshocht, S.; De Gendt, S.; Heyns, M.; Wouters, D.J.; Kittl, J.A. Dielectric response of Ta_2O_5 , Nb_2O_5 , and NbTaO_5 from first-principles investigations. *ECS Trans.* **2009**, *19*, 729–737. [[CrossRef](#)]
14. Gibot, P.; Oudot, F.; Lalle, B.; Schnell, F.; Spitzer, D. Nanosized niobium (V) and tantalum (V) oxide ceramics as competitive oxidizers within aluminum-based nanothermites. *Energetic Mater. Front.* **2021**, *2*, 167–173. [[CrossRef](#)]
15. Singh, B.; Singh, G.; Sidhu, B.S. In vitro investigation of NbTa alloy coating deposited on CoCr alloy for biomedical implants. *Surf. Coat. Technol.* **2019**, *377*, 124932. [[CrossRef](#)]
16. Peltier, L.; Berveiller, S.; Meraghni, F.; Lohmuller, P.; Laheurte, P. Martensite transformation and superelasticity at high temperature of $(\text{TiHfZr})_{74}(\text{NbTa})_{26}$ high-entropy shape memory alloy. *Shape Mem. Superelasticity* **2021**, *7*, 194–205. [[CrossRef](#)]
17. Machad, J.P.B.; Rodrigues, D., Jr.; Rodrigues, C.A. Development of $(\text{Nb,Ta})_3\text{Sn}$ multifilamentary superconductor wire using a novel niobium tube and internal tin method for high current applications. *Phys. C Supercond.* **2004**, *408–410*, 204–206. [[CrossRef](#)]
18. Timms, W.E.; Walmsley, D.G. Magnetic and resistive behavior of a superconducting Nb-54 at.% Ta cylinder. *J. Phys. F Met. Phys.* **1976**, *6*, 2107. [[CrossRef](#)]
19. Jeong, M.; Jung, J.-Y.; Seo, C.-S.; Park, S.-W. Characteristics of an electrochemical reduction of Ta_2O_5 for the preparation of metallic tantalum in a $\text{LiCl-Li}_2\text{O}$ melt. *J. Alloys Compd.* **2007**, *440*, 210–215. [[CrossRef](#)]
20. Wu, T.; Jin, X.; Xiao, W.; Hu, X.; Wang, D.; Chen, G.Z. Fast electrochemical preparation of capacitor grade tantalum powder. *Chem. Mater.* **2007**, *19*, 153–160. [[CrossRef](#)]
21. Yan, X.Y.; Fray, D.J. Production of niobium powder by direct electrochemical reduction of solid Nb_2O_5 in a eutectic CaCl_2 - NaCl melt. *Metall. Mater. Trans. B* **2002**, *33*, 685–693. [[CrossRef](#)]
22. Sure, J.; Vishnu, D.S.M.; Schwandt, C. Direct electrochemical synthesis of high-entropy alloys from metal oxides. *Appl. Mater. Today* **2017**, *9*, 111–121. [[CrossRef](#)]
23. Chorney, M.P. Investigations of Solid-State Sintering Behavior of Binary Refractory Mixed Oxide Systems. Master's Thesis, Montana Tech of the University of Montana, Butte, MT, USA, 2018.
24. Mohanty, G.P.; Fiegel, L.J.; Healy, J.H. On the System Niobium Pentoxide—Tantalum Pentoxide. *J. Phys. Chem.* **1964**, *68*, 208–210. [[CrossRef](#)]
25. Fazio, M.A.; Yang, L.; Menoni, C.S. Prediction of crystallized phases of amorphous Ta_2O_5 -based mixed oxide thin films using a density functional theory database. *APL Mater.* **2021**, *9*, 031106. [[CrossRef](#)]
26. Mohanty, G.P.; Fiegel, L.J.; Healy, J.H. Unit cell and space group of $2\text{Nb}_2\text{O}_5 \cdot \text{Ta}_2\text{O}_5$. *Acta Cryst.* **1962**, *15*, 1190. [[CrossRef](#)]
27. Holtzberg, F.; Reisman, A.; Berry, M.; Berkenblit, M. Chemistry of the group VB pentoxides. VI: The polymorphism of Nb_2O_5 . *J. Am. Chem. Soc.* **1957**, *70*, 2039–2043. [[CrossRef](#)]